Am J Cancer Res 2025;15(6):2750-2764
www.ajcr.us /ISSN:2156-6976/ajcr0162724

Original Article

Identification of CDK2 as a key apoptotic gene for predicting cervical cancer prognosis using bioinformatics and machine learning

Miao-Miao Li[1,2], Min Song[3], Shu-Xia Wu[2], Xing-Ye Ren[4]

[1]*School of Clinical Medicine, Shandong Second Medical University, Weifang 261053, Shandong, China;* [2]*Department of Gynecology and Obstetrics, The Fifth People's Hospital of Jinan, Jinan 250022, Shandong, China;* [3]*Department of Obsteric, Jinan Maternal and Child Care Hospital, Jinan 250001, Shandong, China;* [4]*Department of Gynecology, The Forth Peoples' Hospital of Jinan, Jinan 250031, Shandong, China*

Received December 17, 2024; Accepted June 17, 2025; Epub June 25, 2025; Published June 30, 2025

Abstract: Objectives: This study aimed to identify apoptosis - related genes with diagnostic and prognostic value in cervical cancer (CC) using integrated bioinformatics and machine learning approaches. Methods: Gene expression datasets were obtained from the National Center for Biotechnology Information Gene Expression Omnibus (GEO) and the Cancer Genome Atlas (TCGA), with GSE192897 used as the training set. A total of 451 differentially expressed genes (DEGs) were identified, including 221 upregulated and 230 downregulated genes. Eleven apoptosis - related upregulated DEGs were selected for further analysis using three machine learning algorithms: random forest, logistic regression, and support vector machine. Validation was performed using GSE192897, GSE166466, and TCGA-CESC datasets. Results: Among the evaluated genes, cyclin-dependent kinase 2 (CDK2) consistently achieved an AUC > 0.8 in all three validation datasets and had a weighted sum rank > 10, meeting stringent selection criteria. In a CC mouse model, CDK2 expression was significantly elevated and positively correlated with squamous cell carcinoma antigen, carcinoembryonic antigen, vascular endothelial growth factor, and heparanase. siRNA-mediated knockdown of CDK2 reduced cell proliferation and migration while promoting apoptosis. Mice with high CDK2 expression showed significantly lower 4-week survival rates, indicating poor prognosis. Conclusions: This study identified CDK2 as a key apoptosis - related gene with strong diagnostic and prognostic value in cervical cancer. CDK2 promotes tumor progression and is associated with poor survival, suggesting its potential as a biomarker and therapeutic target for personalized treatment strategies in CC.

Keywords: Cervical cancer, machine learning, bioinformatics, apoptosis, CDK2, diagnosis

Introduction

Despite recent declines in the incidence and mortality rates of cervical cancer (CC), it remains the third most common cancer and the fourth leading cause of cancer - related deaths among women worldwide, particularly in less developed countries [1-3]. Early-stage CC can be effectively treated if diagnosed promptly [4-6]; however, treatment options for advanced or recurrent CC remain limited and largely ineffective [7]. Current standard therapies, including surgical resection, radiotherapy, and chemotherapy, often fail to achieve satisfactory long-term outcomes [8, 9]. Therefore, identifying novel anti-cancer targets is crucial to improving therapeutic efficacy. In addition, there is an urgent need for reliable prognostic biomarkers to enhance the survival outcomes of CC patients.

In recent years, bioinformatics and machine learning have provided new insights into cancer research [10, 11]. These technologies enable the efficient analysis of large-scale gene expression data and facilitate the discovery of diagnostic and prognostic biomarkers. For complex diseases such as CC, integrating bioinformatics with machine learning algorithms can more accurately identify key genes and construct robust predictive models [12]. The use of machine learning has been increasingly adopt-

https://doi.org/10.62347/RUXJ3980

ed in CC risk prediction, diagnosis, and classification. For instance, Mehmood et al. proposed CervDetect, a machine learning-based method for assessing CC risk factors [13]. Park et al. applied the deep learning model ResNet-50 alongside machine learning to identify CC features from cervicography images [14]. Rehimi et al. used machine learning to analyze CC incidence, aiding in diagnosis and prognosis [15]. Although apoptosis - related genes play vital roles in tumor progression, their specific functions and mechanisms in CC remain inadequately understood.

Identifying robust biomarkers for disease progression and individualized treatment is essential to improving CC clinical management. Recent advances in bioinformatics and machine learning have paved the way for identifying key genes and developing predictive models that could transform CC diagnosis and therapy. This study aimed to identify differentially expressed apoptosis - related genes in CC using integrated bioinformatics and machine learning approaches. By uncovering potential prognostic biomarkers, we seek to improve therapeutic strategies and provide novel insights into the molecular mechanisms underlying CC, ultimately contributing to precision medicine in its management.

Materials and methods

Datasets

The datasets GSE192897 and GSE166466 were downloaded from the National Center for Biotechnology Information - Gene Expression Omnibus (GEO) database (https://www.ncbi.nlm.nih.gov/gds/) [16].

GSE192897 was generated using the GPL-27956 NanoString Human nCounter PanCancer IO 360 Panel platform and includes 34 CC samples and 14 healthy controls.

GSE166466 was based on the GPL23126 [Clariom_D_Human] Affymetrix Human Clariom D Assay [transcript (gene) version] platform and contains 7 normal cervical epithelium tissues, 6 HPV16-positive high-grade squamous intraepithelial lesion tissues, and 7 CC tissues.

The Cancer Genome Atlas -Cervical Squamous Cell Carcinoma and Endocervical Adenocarcinoma dataset (TCGA-CESC, https://cancergenome.nih.gov/) comprises 309 tumor samples.

GSE192897 was used as the training set, while GSE166466 and TCGA-CESC served as validation sets for subsequent analyses.

Differentially expressed genes (DEGs) analysis

DEGs between CC and control groups in the GSE192897 dataset were identified using the "limma" package in R. Genes with $|\log_2$ fold change (FC)| > 0.58 and adjusted $P < 0.05$ were considered significant.

Machine learning

Three machine learning algorithms - random forest [17], logistic regression [18], and support vector machine (SVM) [19] - were employed using GSE192897, GSE166466, and TCGA-CESC as test datasets.

Feature weights from the three models were extracted and ranked. Genes with an average area under the curve (AUC) > 0.8 across all datasets and a combined feature weight rank > 10 were selected for further analysis. ROC curves and rank statistics were used to assess model performance and gene importance.

Animal model

Eighty female mice (6-8 weeks old, 20 ± 2 g) were housed under standard conditions with ad libitum access to food and water. All procedures complied with the Regulations for the Administration of Affairs Concerning Experimental Animals.

Forty mice were randomly selected for modeling. U14 cells in the logarithmic growth phase were harvested and resuspended in sterile normal saline to a final concentration of 5×10^6 cells/mL. To ensure consistency and reproducibility of the CC model, this procedure was repeated for three consecutive passages: cells were collected from the peritoneal cavities of tumor-bearing mice, expanded in culture, and re-injected into new mice following the same protocol.

After the third passage, 0.2 mL of the cell suspension (containing 1 × 10^6 cells) was subcutaneously injected into the right axilla of each mouse to establish the U14 cervical cancer mouse model.

Animal euthanasia

Mice were euthanized by CO_2 inhalation (flow rate: 20% chamber volume/min), followed by cervical dislocation to ensure death, in accordance with institutional animal care guidelines.

Ethics statement

All animal experiments were approved by the Ethics Committee of The Fifth People's Hospital of Jinan Affiliated to Shandong Second Medical University. Efforts were made to minimize animal suffering throughout the study.

Cell culture

HeLa and CaSki CC cell lines were cultured in DMEM (Hyclone, #SH30243.01B) supplemented with 10% fetal bovine serum (Hyclone, #SH30084.03), and seeded in 6-well plates (5 × 10^5 cells/well) in a 37°C incubator with 5% CO_2.

Cell transfection

HeLa and CaSki cells were seeded in 96-well plates (1 × 10^4 cells/well) and incubated for 24 h. Transfection was performed using 3 pmol si-CDK2 or negative control siRNA (si-NC) (Shanghai GenePharma Co., Ltd) and 0.3 μL Lipofectamine 2000 (Invitrogen, #52887). siRNA and transfection reagent were diluted in 5 μL of culture medium, mixed, incubated at room temperature for 10 min, and added to each well. RT-qPCR was used to verify transfection efficiency after 48 h. siRNA sequences are listed in Table S1.

RT-qPCR

Total RNA was extracted with TRIzol (Invitrogen) and reverse transcribed into cDNA (Takara, China). RT-qPCR was performed using SYBR® Premix Ex Taq™ (Takara) on an ABI7300 system. Relative expression was calculated using the 2^-ΔΔCt method, with β-actin as the internal control.

Primer sequences: β-actin: Forward 5'-TCACCAACTGGGACGACATG-3', Reverse 5'-AGTCCTGTGGCATCCACGAA-3'. CDK2: Forward 5'-CCAGTACTGCCATCCGAGAG-3', Reverse 5'-CGGCGAGTCACCATCTCAGC-3'.

Western blot (WB)

Proteins were extracted using RIPA buffer (Sigma-Aldrich) and quantified with a BCA kit (Thermo Scientific). Equal protein amounts were separated by SDS-PAGE and transferred to PVDF membranes (Millipore). After blocking in 5% milk, membranes were incubated overnight at 4°C with primary antibodies:

CDK2 (#GB12237, 1:1000), Caspase 3 (#GB11767C, 1:1000), BCL-2 (#GB124830, 1:1000), BAX (#GB12690, 1:1000), GAPDH (#GB15002, 1:2000) (all from Servicebio).

The next day, membranes were incubated with HRP-conjugated secondary antibody (#GB23303, 1:3000) for 1 h at room temperature. Signal detection was performed using the AIWBwell™ ECL system (Servicebio).

Enzyme-linked immunosorbent assay (ELISA) assay

Levels of squamous cell carcinoma antigen (SCCA), carcinoembryonic antigen (CEA), vascular endothelial growth factor (VEGF) and heparanase (HPA) were measured using ELISA kits (R&D Systems, USA). Assays were performed according to manufacturer protocols. Absorbance was measured at 450-570 nm using a microplate reader (BioTek ELX 800, USA).

Cell counting kit-8 (CCK-8) assay

Transfected cells (1 × 10^4 cells/well) were seeded into 96-well plates. At 24, 48, 72, and 96 h, 10 μL of CCK-8 reagent (Beyotime, #C0038) was added to each well. Plates were incubated for 1 h at 37°C in the dark, and absorbance was measured at 450 nm using a microplate reader. Each experiment was repeated at least three times.

Scratch assay

Cells were seeded in 6-well plates (1 × 10^6 cells/mL). Once confluent, scratches were made using a sterile 200 μL pipette tip. Cells were washed with PBS, and wound closure was

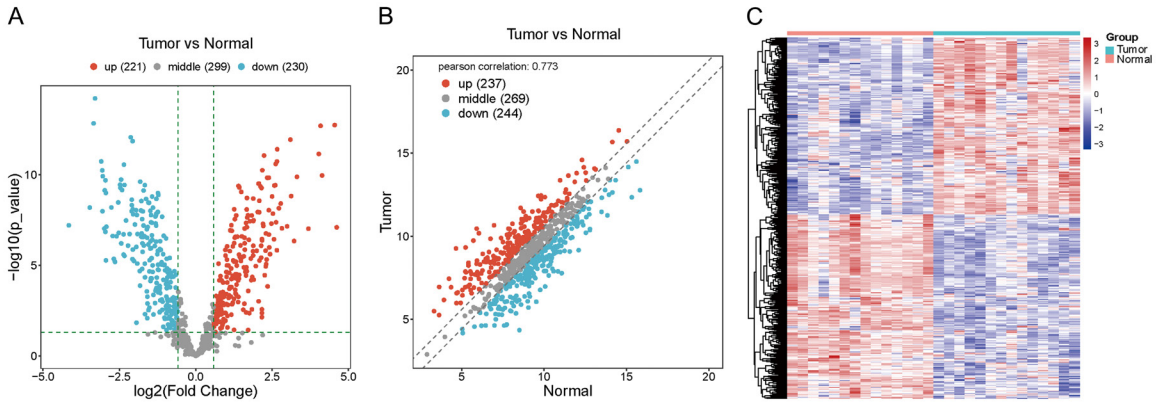

Figure 1. Identification of the differentially expressed genes between cervical cancer group and normal group from the training set GSE192897. A. Volcano plot; B. Scatter plot; C. Heat map. The red dots indicate the upregulated genes and the blue dots indicate the downregulated genes.

imaged at 0, 24, and 48 h under a microscope. Each experiment was independently repeated three times.

Statistical analysis

All data were analyzed using R (v3.5.2) or GraphPad Prism (v9.0.1). Results are presented as mean ± standard deviation (SD). Student's t-test or Wilcoxon test was used for two-group comparisons. For multi-group comparisons, one-way or repeated-measures ANOVA followed by Tukey's HSD or Bonferroni correction was applied. Pearson correlation was used for correlation analysis. Kaplan-Meier analysis was performed for survival comparisons. A *P*-value < 0.05 was considered statistically significant.

Results

Screening of dysregulated genes

Using the threshold criteria of $|\log_2 FC| > 0.58$ and adjusted $P < 0.05$, a total of 451 DEGs were identified from the GSE192897 dataset, including 221 upregulated and 230 downregulated genes. The DEGs, along with their corresponding fold changes and adjusted *P*-values, are presented in Table S2. Additionally, a volcano plot, scatter plot, and heatmap were generated for visualization (**Figure 1A-C**).

Constuction and validation of an apoptosis-related gene model

Eleven apoptosis-related genes-CASP8, TNFSF10, FASLG, IRF1, CASP1, CD38, CDK2, TAP1, BRCA1, CD14, and ERBB2-were selected from the upregulated DEGs to assess their prognostic value in CC (**Figure 2A-K**). These genes were used to construct prediction models using random forest, logistic regression, and linear SVM algorithms. All three algorithms achieved an AUC of 1 during cross-validation (**Figure 3A**). Consistent results were obtained in individual algorithm analyses (**Figure 3B**). The feature importance rankings for each algorithm are summarized in Table S3. Except for CASP1, CD38, and FASLG, the weight rank sum of the remaining genes exceeded 10.

To further validate diagnostic accuracy, ROC curve analyses were performed. CASP1, CASP8, CDK2, and TNFSF10 demonstrated AUCs > 0.7 across all three datasets (**Figure 4A-K**). To ensure robust and clinically relevant results, genes with AUC > 0.8 across all datasets and a weight rank sum > 10 were considered for further analysis. Only CDK2 satisfied these stringent criteria, highlighting its diagnostic potential and stability across datasets.

Elevated CDK2 expression promotes CC progression

To validate the diagnostic utility of CDK2, its expression and correlation with CC markers (SCCA, CEA, VEGF, and HPA) were examined in CC and normal mice using WB, RT-qPCR, and ELISA. In CC mice, CDK2 mRNA and protein expression levels were significantly elevated, as were protein levels of all four markers (**Figure 5A-F**). Correlation analyses revealed strong positive associations between CDK2

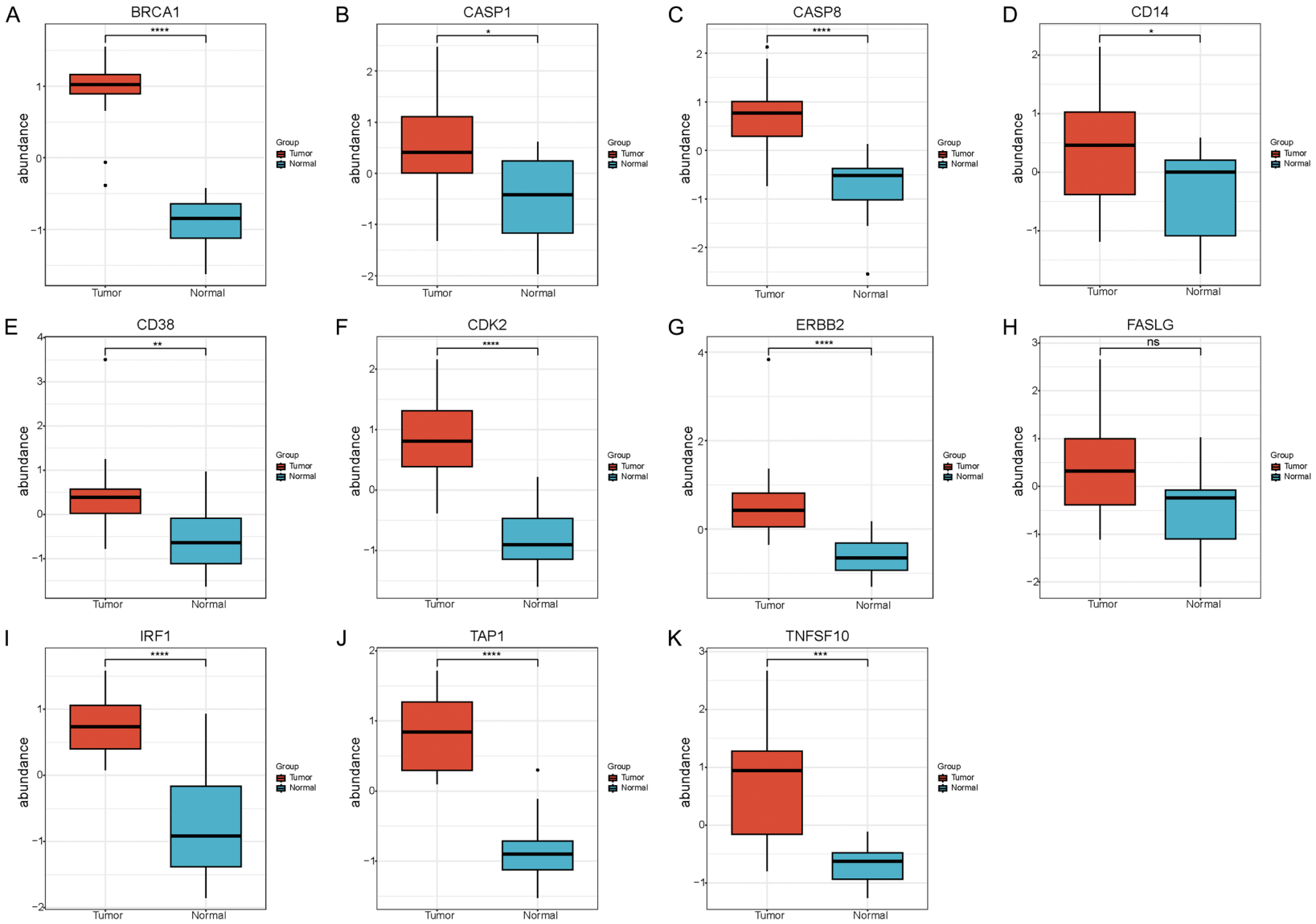

Figure 2. The apoptotic Characteristic genes between the cervical cancer group and the normal group in the training set GSE192897. A-K. The box plot shows the expression of the genes in the training set between the cervical cancer group and normal group. Red box indicates the cervical cancer group, and blue indicates the normal group. *P < 0.05, **P < 0.01, ***P < 0.001, ****P < 0.0001 and ns, no significance. BRCA1: Breast Cancer gene 1; CASP1: Caspase 1; CASP8: Caspase

8; CD14: Cluster of Differentiation 14; CD39: Ectonucleoside Triphosphate Diphosphohydrolase 1; CDK2: Cyclin-dependent kinase 2; ERBB2: Erb-B2 Receptor Tyrosine Kinase 2; FASLG: Fas Ligand; IRF1: Interferon Regulatory Factor 1; TAP1: Transporter associated with Antigen Processing 1; TNFSF10: Tumor Necrosis Factor Superfamily member 10.

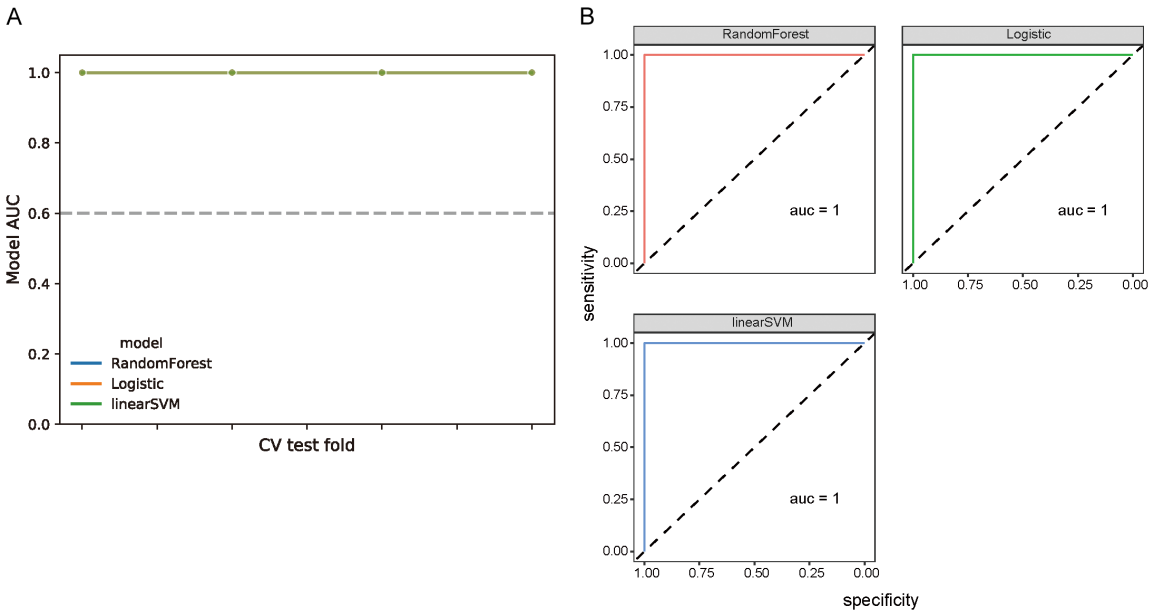

Figure 3. The machine learning of the eleven apoptosis related genes by random forest, logistic regression and linear SVM algorithms. A. Cross-validation. B. Independent verification of the three algorithms. AUC: Area Under the Curve; CV: Cross-Validation; SVM: Support Vector Machine.

and SCCA (r = 0.986, P < 0.001), CEA (r = 0.979, P < 0.001), VEGF (r = 0.979, P < 0.001), and HPA (r = 0.986, P < 0.001) (**Figure 6**), suggesting that CDK2 may play a key role in CC development. The immune cells infiltration between tumor and normal groups are summarized in Table S4.

Effects of CDK2 knockdown on proliferation, apoptosis, and migration of CC cells

To explore the functional role of CDK2, three siRNAs targeting CDK2 were transfected into Hela and Caski cells. Knockdown of CDK2 significantly upregulated pro-apoptotic genes (BAX, CASP3) and downregulated anti-apoptotic BCL-2 (**Figure 7**). CCK-8 assays revealed that CDK2 knockdown impaired the proliferative capacity of CC cells (**Figure 8**). Additionally, scratch assays showed significantly reduced migration rates in CDK2-silenced cells at 24 h and 48 h (**Figure 9**). These results indicate that CDK2 is crucial for promoting CC cell proliferation and migration and for inhibiting apoptosis.

CDK2 expression and 4-Week survival in CC mice

Based on the optimal cutoff value of CDK2 expression (20.38), 20 mice were assigned to the high-expression group (CDK2 ≥ 20.38), and 20 to the low-expression group (CDK2 < 20.38). Kaplan-Meier survival analysis demonstrated that the 4-week survival rate of the high-expression group (15.0%) was significantly lower than that of the low-expression group (45.0%) (**Figure 10**).

Discussion

In 2020, over 600,000 new cases of CC were diagnosed worldwide, resulting in nearly 340,000 deaths among women [20]. Identifying target genes and effective therapeutics is crucial to improving survival rates and reducing mortality in CC. By analyzing multiple CC datasets from various public databases, this study has enhanced our understanding of the molecular mechanisms underlying CC and identified key diagnostic genes. The importance of these

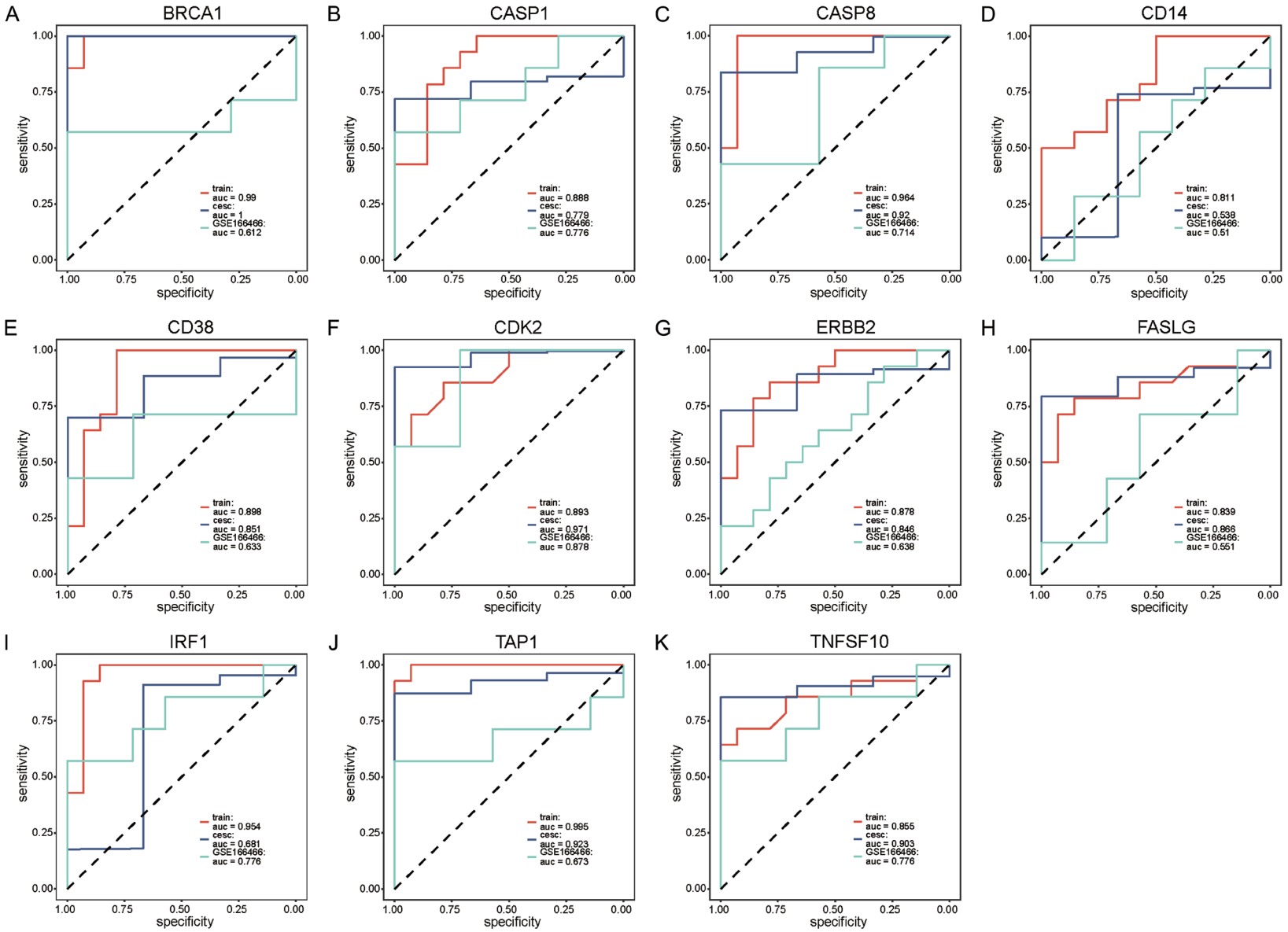

Figure 4. ROC curves of the cervical cancer group in GSE192897, GSE166466 and TCGA- CC. A-K. The figures show the ROC curve of eleven apoptosis related genes in the training set. The abscissa is the false positive rate, which is represented by 1-specificity, and the ordinate is the true positive rate, which is represented

by sensitivity. ROC: receiver operation characteristic; TCGA: The Cancer Genome Atlas; BRCA1: Breast Cancer gene 1; CASP1: Caspase 1; CASP8: Caspase 8; CD14: Cluster of Differentiation 14; CD39: Ectonucleoside Triphosphate Diphosphohydrolase 1; CDK2: Cyclin-dependent kinase 2; ERBB2: Erb-B2 Receptor Tyrosine Kinase 2; FASLG: Fas Ligand; IRF1: Interferon Regulatory Factor 1; TAP1: Transporter associated with Antigen Processing 1; TNFSF10: Tumor Necrosis Factor Superfamily member 10.

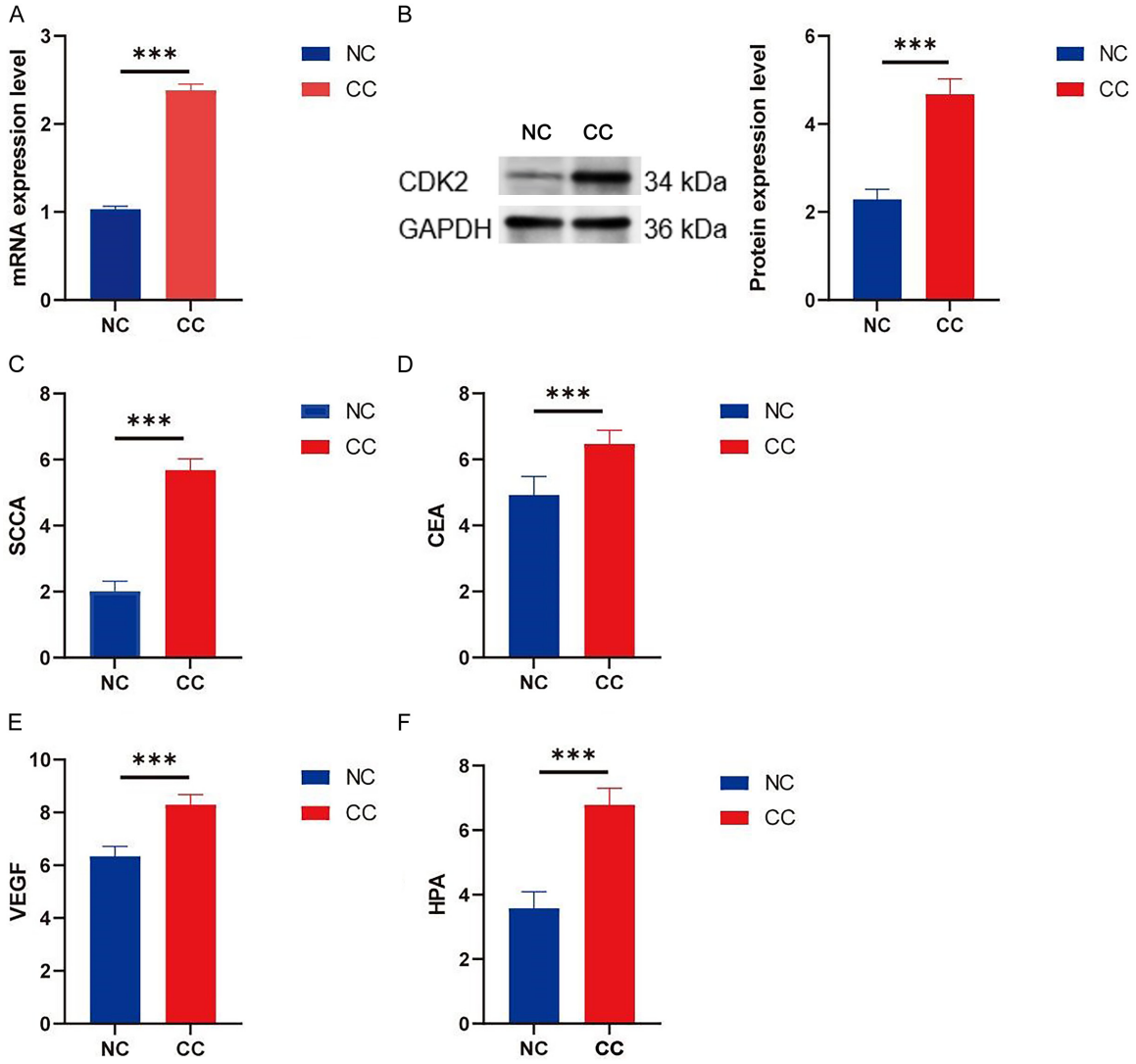

Figure 5. Increased expression of CDK2 promotes the development of cervical cancer. A. RT-qPCR of CDK2 mRNA expression. B. Western Blot analysis of the CDK2 protein expression. C-F. ELISA of the SCCA, CEA, VEGF, and HPA protein expression. ***P < 0.001 between normal control group and cervical cancer group. NC: normal control; CC: cervical cancer; mRNA: messenger RNA; CDK2: Cyclin-dependent kinase 2; GAPDH: Glyceraldehyde-3-phosphate dehydrogenase; SCCA: Squamous cell carcinoma antigen; CEA: Carcinoembryonic antigen; VEGF: Vascular endothelial growth factor; HPA: Human placental alkaline phosphatase; RT-qPCR: Real-time quantitative polymerase chain reaction; ELISA: Enzyme-linked immunosorbent assay.

findings lies in the potential use of candidate genes for early intervention, potentially preventing progression to malignant disease. A total of 451 DEGs were identified from the GSE192897 dataset. Further analysis revealed that 11 apoptosis-related genes-including CASP8, TNFSF10, FASLG, IRF1, CASP1, CD38, CDK2, TAP1, BRCA1, CD14, and ERBB2 - were significantly upregulated in CC.

Despite advances in treatment, the prognosis of CC remains suboptimal, especially due to

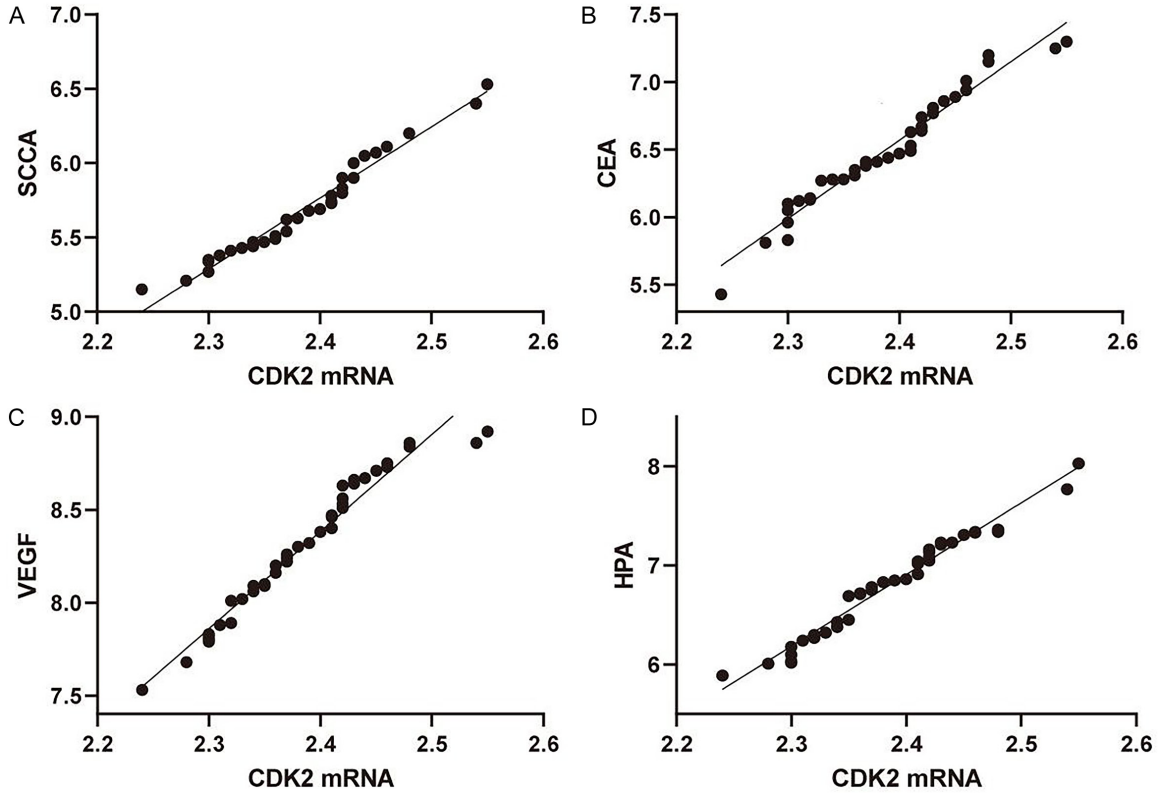

Figure 6. Analysis of the correlation between CDK2 mRNA expression levels and CC markers. A. The correlation between CDK2 mRNA and SCCA; B. The correlation between CDK2 mRNA and CEA; C. The correlation between CDK2 mRNA and VEGF; D. The correlation between CDK2 mRNA and HPA. CC: cervical cancer; SCCA: Squamous Cell Carcinoma Antigen; CEA: Carcinoembryonic Antigen; VEGF: Vascular Endothelial Growth Factor; HPA: Human Placental Alkaline Phosphatase; mRNA: messenger RNA; CDK2: Cyclin-dependent kinase 2.

stark differences in survival between early and advanced stages [21-23]. Reliable and efficient diagnostic models are still lacking. In this study, apoptosis-related gene models were constructed using random forest, logistic regression, and linear SVM algorithms. CDK2, with an AUC > 0.8 and a weighted rank sum > 10, was identified as a candidate gene. This multi-model comparison approach enhances the robustness of the findings and provides diverse perspectives on the biological role of CDK2 in CC. CDK2, a member of the cyclin-dependent kinase family, plays a pivotal role in the regulation of the eukaryotic cell cycle [24-26]. Previous studies have implicated CDK2-related signaling pathways in CC progression [27-29], and elevated CDK2 expression in CC tissues has been shown to promote tumor progression [30, 31]. Notably, CDK2 consistently emerged as a key feature across all three models and datasets, reinforcing its potential as a reliable predictive biomarker.

siRNA-mediated knockdown of CDK2 significantly inhibited the proliferation and migration of CC cells, while upregulating pro-apoptotic genes BAX and CASP3. These results support the notion that CDK2 is not only a regulator of the cell cycle but also a modulator of cell survival signaling pathways [27, 28]. Therefore, CDK2-targeted small-molecule inhibitors or RNA interference strategies may offer promising therapeutic options for CC. Moreover, high CDK2 expression was closely associated with poor prognosis, suggesting its involvement in CC progression.

Survival analysis further confirmed CDK2 as an independent prognostic factor. Compared with the low-expression group, mice in the high-expression group exhibited significantly lower 4-week survival rates, highlighting the critical role of CDK2 in CC pathophysiology. Given the current scarcity of effective biomarkers to guide personalized treatment strategies in clin-

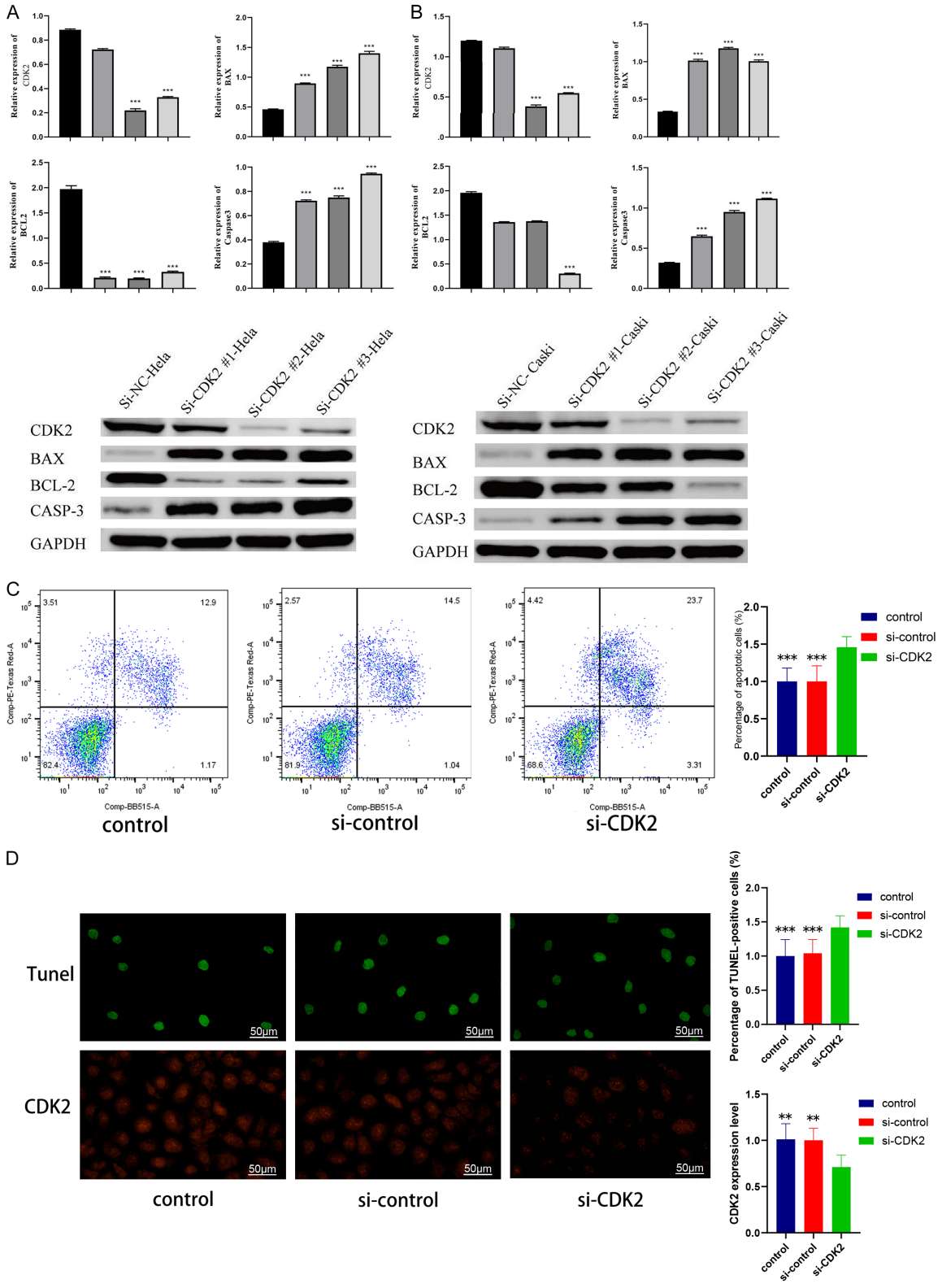

Figure 7. Knockdown of CDK2 promotes apoptosis of cervical cancer cells. A. Western Blot analysis of Hela cells showing the expression levels of CDK2, BAX, BCL-2, and CASP-3 after knockdown of CDK2, ***P < 0.001 compared to si-NC group; B. Western Blot analysis of Caski cells showing the expression levels of CDK2, BAX, BCL-2, and CASP-3 after knockdown of CDK2, ***P < 0.001 compared to si-NC group; C. Flow cytometry analysis of cervical cancer cells stained with Annexin V-FITC and PI for detecting apoptotic cells, ***P < 0.001 compared to si-CDK2 group; D.

TUNEL staining combined with CDK2 fluorescence Co-staining to detect TUNEL-positive cells and CDK2 expression in cervical cancer cells (20×), **P < 0.01, ***P < 0.001 compared to si-CDK2 group. Si-NC: Small interfering RNA negative control; CDK2: Cyclin-dependent kinase 2; Si-CDK2: Small interfering RNA targeting CDK2; BAX: BCL2-associated X protein; BCL-2: B-cell lymphoma 2; CASP-3: Caspase 3; GAPDH: Glyceraldehyde-3-phosphate dehydrogenase; TUNEL: Terminal deoxynucleotidyl transferase dUTP nick end labeling; V-FITC: V-Fluorescein isothiocyanate; PI: Propidium Iodide.

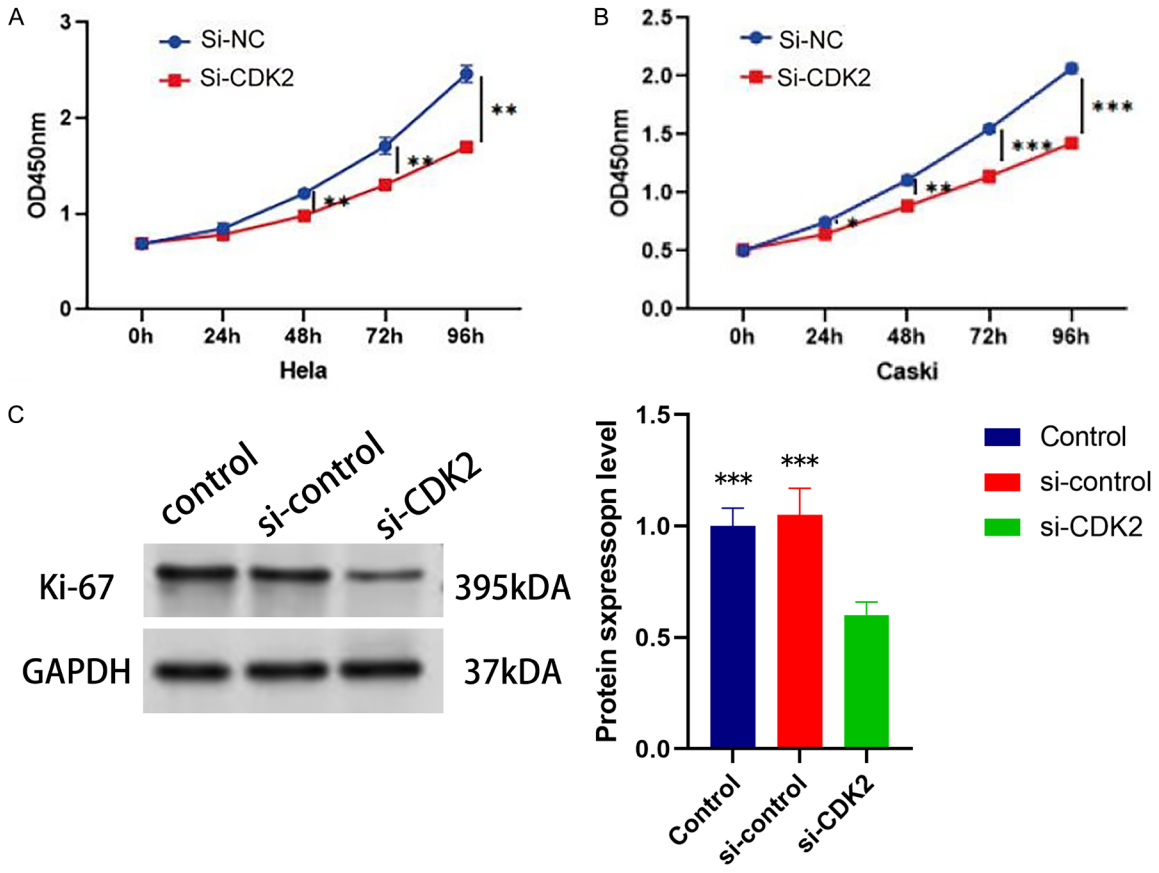

Figure 8. Knockdown of CDK2 attenuates proliferation of cervical cancer cells. A. CCK-8 assays of the proliferative capacity in CDK2-knockdown Hela cells, **P < 0.01 compared to 0 h; B. CCK-8 assays of the proliferative capacity in CDK2-knockdown Caski cells, *P < 0.05, **P < 0.01, ***P < 0.001 compared to 0 h; C. Western Blot analysis of Ki-67 expression in cervical cancer cells, ***P < 0.001 compared to si-CDK2 group. Si-NC: Small interfering RNA negative control; CDK2: Cyclin-dependent kinase 2; Si-CDK2: Small interfering RNA targeting CDK2; OD450 nm: Optical Density at 450 nanometers; Ki-67: Antigen identified by monoclonal antibody Ki-67; GAPDH: Glyceraldehyde-3-phosphate dehydrogenase.

ical practice, our findings provide both theoretical and methodological support for the development of novel diagnostic and therapeutic approaches.

While integrating bioinformatics and machine learning has facilitated the identification of diagnostically relevant genes in CC, this study has several limitations. First, the limited sample size may affect the generalizability of the findings. Second, although the function of CDK2 was validated in vitro and in animal models, its precise mechanism in humans remains unclear. Third, the interaction network between CDK2 and other molecular targets has not been fully elucidated. Future studies will expand the sample size, conduct prospective cohort studies, and explore the feasibility of CDK2 as a therapeutic target. In particular, additional work will aim to clarify its interaction networks and validate its translational potential in clinical settings.

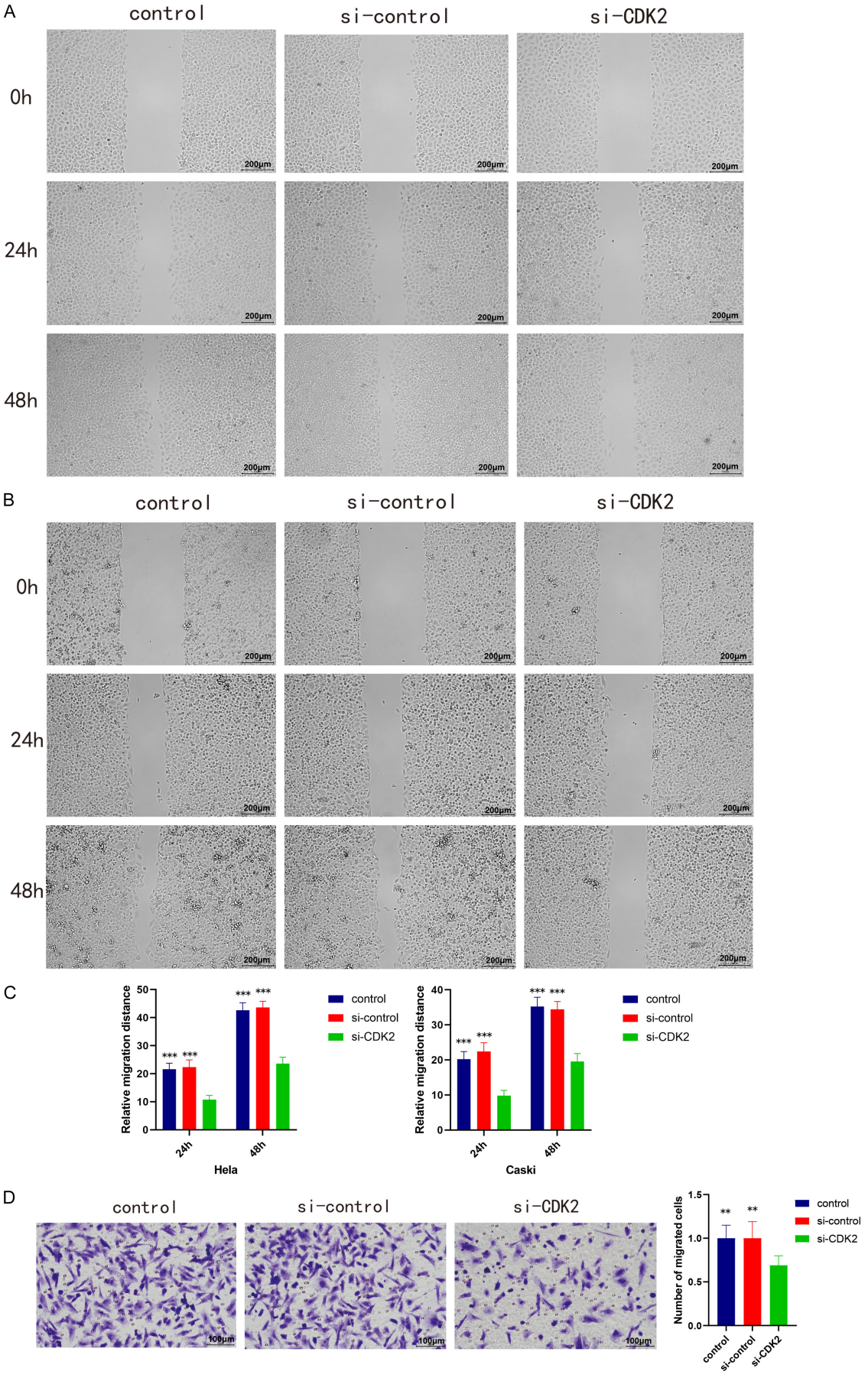
A
control
si-control
si-CDK2
0h
24h
48h
200μm
B
control
si-control
si-CDK2
0h
24h
48h
200μm
C
Relative migration distance
control
si-control
si-CDK2
***
24h
48h
Hela
Caski
D
control
si-control
si-CDK2
100μm
Number of migrated cells
**

Figure 9. Knockdown of CDK2 attenuates migration of cervical cancer cells. A. Cell scratch assay of Hela cells to assess cell migration (10×); B. Cell scratch assay of Caski cells to assess cell migration (10×); C. Relative migration distance for both Hela and Caski cells, ***P < 0.001 compared to si-CDK2 group; D. Transwell migration assay to detect the number of migrated cells (20×), **P < 0.01 compared to si-CDK2 group. CDK2: Cyclin-dependent kinase 2; Si-CDK2: Small interfering RNA targeting CDK2.

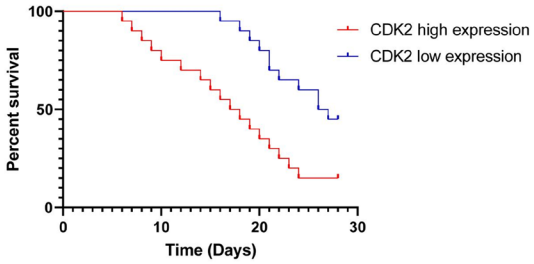

Figure 10. CDK2 expression and kaplan-meier survival curves of 4-week survival prognosis in cervical cancer mice. CDK2: Cyclin-dependent kinase 2.

While this study has provided substantial evidence for the role of CDK2 in CC progression, one important question remains unresolved: the impact of CDK2 on cell migration and invasion. Due to limitations in the current experimental design, we were unable to perform transwell assays to directly assess these properties. Future research will address this limitation by incorporating transwell migration and invasion assays to evaluate the functional consequences of CDK2 modulation in CC cells. This will be critical for a more comprehensive understanding of CDK2's oncogenic role and its value as a therapeutic target.

In summary, this study integrated bioinformatics and machine learning to construct an apoptosis-related gene signature model. We identified CDK2 as a robust diagnostic and prognostic biomarker and validated its biological role in cervical cancer through both in vitro and in vivo analyses. These findings lay a solid foundation for the development of CDK2-targeted diagnostic tools and therapeutic interventions, with the ultimate goal of improving clinical outcomes for patients with cervical cancer.

Acknowledgements

This work was supported by Jinan Municipal Health Commission Science and Technology Plan Project (2022-2-84), and Shandong Province Medical Health Science and Technology Plan Project (202405010786).

Disclosure of conflict of interest

None.

Address correspondence to: Xing-Ye Ren, Department of Gynecology, The Forth Peoples' Hospital of Jinan, Jinan 250031, Shandong, China. E-mail: wuyuanrenxingye@163.com; Shu-Xia Wu, Department of Gynecology and Obstetrics, The Fifth People's Hospital of Jinan, Jinan 250022, Shandong, China. E-mail: 13791033207@163.com

References

[1] Chargari C, Peignaux K, Escande A, Renard S, Lafond C, Petit A, Lam Cham Kee D, Durdux C and Haie-Méder C. Radiotherapy of cervical cancer. Cancer Radiother 2022; 26: 298-308.

[2] Caruso G, Wagar MK, Hsu HC, Hoegl J, Rey Valzacchi GM, Fernandes A, Cucinella G, Sahin Aker S, Jayraj AS, Mauro J, Pareja R and Ramirez PT. Cervical cancer: a new era. Int J Gynecol Cancer 2024; 34: 1946-1970.

[3] Noor Mohamad NA and Omar J. Cervical cancer in Malaysia. J Obstet Gynaecol Res 2024; 50 Suppl 1: 49-54.

[4] Voelker RA. Cervical cancer screening. JAMA 2023; 330: 2030.

[5] Sahasrabuddhe VV. Cervical cancer: precursors and prevention. Hematol Oncol Clin North Am 2024; 38: 771-781.

[6] Yadav G, Srinivasan G and Jain A. Cervical cancer: novel treatment strategies offer renewed optimism. Pathol Res Pract 2024; 254: 155136.

[7] Yang HJ, Xue JM, Li J, Wan LH and Zhu YX. Identification of key genes and pathways of diagnosis and prognosis in cervical cancer by bioinformatics analysis. Mol Genet Genomic Med 2020; 8: e1200.

[8] Abu-Rustum NR, Yashar CM, Arend R, Barber E, Bradley K, Brooks R, Campos SM, Chino J, Chon HS, Crispens MA, Damast S, Fisher CM, Frederick P, Gaffney DK, Gaillard S, Giuntoli R, Glaser S, Holmes J, Howitt BE, Lea J, Mantia-Smaldone G, Mariani A, Mutch D, Nagel C, Nekhlyudov L, Podoll M, Rodabaugh K, Salani R, Schorge J, Siedel J, Sisodia R, Soliman P, Ueda S, Urban R, Wyse E, McMillian NR, Aggarwal S and Espinosa S. NCCN Guidelines®

insights: cervical cancer, version 1.2024. J Natl Compr Canc Netw 2023; 21: 1224-1233.
[9] Sharma S, Deep A and Sharma AK. Current treatment for cervical cancer: an update. Anticancer Agents Med Chem 2020; 20: 1768-1779.
[10] Luo W. Predicting cervical cancer outcomes: statistics, images, and machine learning. Front Artif Intell 2021; 4: 627369.
[11] Wu B and Xi S. Bioinformatics analysis of differentially expressed genes and pathways in the development of cervical cancer. BMC Cancer 2021; 21: 733.
[12] Al Mudawi N and Alazeb A. A model for predicting cervical cancer using machine learning algorithms. Sensors (Basel) 2022; 22: 4132.
[13] Mehmood M, Rizwan M, Gregus Ml M and Abbas S. Machine learning assisted cervical cancer detection. Front Public Health 2021; 9: 788376.
[14] Park YR, Kim YJ, Ju W, Nam K, Kim S and Kim KG. Comparison of machine and deep learning for the classification of cervical cancer based on cervicography images. Sci Rep 2021; 11: 16143.
[15] Rahimi M, Akbari A, Asadi F and Emami H. Cervical cancer survival prediction by machine learning algorithms: a systematic review. BMC Cancer 2023; 23: 341.
[16] de Geus V, Ewing-Graham PC, de Koning W, de Koning MNC, van den Bosch TPP, Nigg AL, van Eijck CHJ, Jozwiak M, van Beekhuizen HJ and Mustafa DAM. Identifying molecular changes in early cervical cancer samples of patients that developed metastasis. Front Oncol 2022; 11: 715077.
[17] Alakus C, Larocque D and Labbe A. Covariance regression with random forests. BMC Bioinformatics 2023; 24: 258.
[18] Dreiseitl S and Ohno-Machado L. Logistic regression and artificial neural network classification models: a methodology review. J Biomed Inform 2002; 35: 352-359.
[19] Wu J and Yang H. Linear regression-based efficient SVM learning for large-scale classification. IEEE Trans Neural Netw Learn Syst 2015; 26: 2357-2369.
[20] Buskwofie A, David-West G and Clare CA. A review of cervical cancer: incidence and disparities. J Natl Med Assoc 2020; 112: 229-232.
[21] Salvo G, Flores Legarreta A, Ramalingam P, Jhingran A, Bhosale P, Saab R, Gonzales NR, Chisholm GB and Frumovitz M. Clinicopathologic characteristics, oncologic outcomes, and prognostic factors in neuroendocrine cervical carcinoma: a neuroendocrine cervical tumor registry study. Int J Gynecol Cancer 2023; 33: 1359-1369.
[22] Cohen CM, Wentzensen N, Castle PE, Schiffman M, Zuna R, Arend RC and Clarke MA. Racial and ethnic disparities in cervical cancer incidence, survival, and mortality by histologic subtype. J Clin Oncol 2023; 41: 1059-1068.
[23] Nitecki R, Ramirez PT, Frumovitz M, Krause KJ, Tergas AI, Wright JD, Rauh-Hain JA and Melamed A. Survival after minimally invasive vs open radical hysterectomy for early-stage cervical cancer: a systematic review and meta-analysis. JAMA Oncol 2020; 6: 1019-1027.
[24] Arora M, Moser J, Hoffman TE, Watts LP, Min M, Musteanu M, Rong Y, Ill CR, Nangia V, Schneider J, Sanclemente M, Lapek J, Nguyen L, Niessen S, Dann S, VanArsdale T, Barbacid M, Miller N and Spencer SL. Rapid adaptation to CDK2 inhibition exposes intrinsic cell-cycle plasticity. Cell 2023; 186: 2628-2643, e21.
[25] Freeman-Cook K, Hoffman RL, Miller N, Almaden J, Chionis J, Zhang Q, Eisele K, Liu C, Zhang C, Huser N, Nguyen L, Costa-Jones C, Niessen S, Carelli J, Lapek J, Weinrich SL, Wei P, McMillan E, Wilson E, Wang TS, McTigue M, Ferre RA, He YA, Ninkovic S, Behenna D, Tran KT, Sutton S, Nagata A, Ornelas MA, Kephart SE, Zehnder LR, Murray B, Xu M, Solowiej JE, Visswanathan R, Boras B, Looper D, Lee N, Bienkowska JR, Zhu Z, Kan Z, Ding Y, Mu XJ, Oderup C, Salek-Ardakani S, White MA, VanArsdale T and Dann SG. Expanding control of the tumor cell cycle with a CDK2/4/6 inhibitor. Cancer Cell 2021; 39: 1404-1421, e11.
[26] Tadesse S, Anshabo AT, Portman N, Lim E, Tilley W, Caldon CE and Wang S. Targeting CDK2 in cancer: challenges and opportunities for therapy. Drug Discov Today 2020; 25: 406-413.
[27] Gerosa R, De Sanctis R, Jacobs F, Benvenuti C, Gaudio M, Saltalamacchia G, Torrisi R, Masci G, Miggiano C, Agustoni F, Pedrazzoli P, Santoro A and Zambelli A. Cyclin-dependent kinase 2 (CDK2) inhibitors and others novel CDK inhibitors (CDKi) in breast cancer: clinical trials, current impact, and future directions. Crit Rev Oncol Hematol 2024; 196: 104324.
[28] Wu J, Chen Y, Li R, Guan Y, Chen M, Yin H, Yang X, Jin M, Huang B, Ding X, Yang J, Wang Z, He Y, Wang Q, Luo J, Wang P, Mao Z, Huen MSY, Lou Z, Yuan J and Gong F. Synergistic anticancer effect by targeting CDK2 and EGFR-ERK signaling. J Cell Biol 2024; 223: e202203005.
[29] Zhang J, Gan Y, Li H, Yin J, He X, Lin L, Xu S, Fang Z, Kim BW, Gao L, Ding L, Zhang E, Ma X, Li J, Li L, Xu Y, Horne D, Xu R, Yu H, Gu Y and Huang W. Inhibition of the CDK2 and Cyclin A complex leads to autophagic degradation of CDK2 in cancer cells. Nat Commun 2022; 13: 2835.

[30] Qu X, Zhu L, Song L and Liu S. Circ_0084927 promotes cervical carcinogenesis by sponging miR-1179 that suppresses CDK2, a cell cycle-related gene. Cancer Cell Int 2020; 20: 333.

[31] Zheng Q, Zhang J, Zhang T, Liu Y, Du X, Dai X and Gu D. Hsa_circ_0000520 overexpression increases CDK2 expression via miR-1296 to facilitate cervical cancer cell proliferation. J Transl Med 2021; 19: 314.

Table S1. The sequence of materials used to regulate gene expression

HYKY-250220039-RNAC			
Gene ID	362817		
siRNA Sequences	Cdk2-rat-778	CGGAGCUUGUUAUCUCAAATT	UUUGAGAUAACAAGCUCCGTT
	Cdk2-rat-526	GGCUGCAAGUACUACUCCATT	UGGAGUAGUACUUGCAGCCTT
	Cdk2-rat-430	GCUGACUUUGGACUAGCAATT	UUGCUAGUCCAAAGUCAGCTT
	si-NC	UUCUCCGAACGUGUCACGUTT	ACGUGACACGUUCGGAGAATT

Notes: siRNA: Small interfering RNA; si-NC: Small interfering RNA negative control.

Table S3. The features weight rank of the genes in the three algorithms

Features	RandomForest	linearSVM	Logistic	rank_sum
BRCA1	11	11	11	33
CDK2	9	10	10	29
IRF1	8	7	9	24
CASP8	7	8	8	23
TAP1	10	4	7	21
ERBB2	6	6	6	18
CD14	3	9	4	16
TNFSF10	5	5	5	15
CASP1	2	3	3	8
CD38	4	2	2	8
FASLG	1	1	1	3

Notes: BRCA1: BReast CAncer gene 1; CDK2: Cyclin-Dependent Kinase 2; IRF1: Interferon Regulatory Factor 1; CASP8: CASPase 8; TAP1: Transporter Associated with Antigen Processing 1; ERBB2: Erb-B2 Receptor Tyrosine Kinase 2; CD14: Cluster of Differentiation 14; TNFSF10: Tumor Necrosis Factor SuperFamily member 10; CASP1: CASPase 1; CD38: Cluster of Differentiation 38; FASLG: FAS Ligand.

Table S4. The immune cells infiltration between tumor and normal groups

Cell	Tumor	Normal	*p* value
B cells memory	0.053348685	0.049285164	1
B cells naive	0.001812735	0.001244774	1
Dendritic cells activated	0.014161804	0.010424008	0.905678116
Dendritic cells resting	0.061394859	0.130893725	0.060750543
Eosinophils	0.07401381	0.038477702	0.01088688
Macrophages M0	0.035562003	0	0.000195088
Macrophages M1	0.142335333	0.012029011	1.65E-05
Macrophages M2	0.004499591	0.031610017	0.020336921
Mast cells activated	0.031457446	0.232872548	0.000110466
Mast cells resting	0.052543681	0.101665549	0.962496015
Monocytes	0.020400542	0.01388894	0.729139833
Neutrophils	0.066326077	0.042949977	0.415937626
NK cells activated	0.041855002	0.025991741	0.122715047
NK cells resting	0.009005809	0.001604538	0.637974142
Plasma cells	0.010343176	0.008113166	0.637974142
T cells CD4 memory activated	0.005569821	0	0.079463849
T cells CD4 memory resting	0.105955033	0.064896279	0.278924863
T cells CD4 naive	0	0.032833787	0.017624587
T cells CD8	0.164238305	0.179385472	0.803612769
T cells follicular helper	0.05678301	0.008974855	0.000642719
T cells gamma delta	0.006713041	0.003853098	1
T cells regulatory (Tregs)	0.04168024	0.00900565	0.002718939

Notes: CD8: Cluster of Differentiation 8; CD4: Cluster of Differentiation 4; NK cells: Natural Killer cells; Tregs: T regulatory cells.